IEEE Access
Multidisciplinary ⋮ Rapid Review ⋮ Open Access Journal

Received 10 July 2024, accepted 2 August 2024, date of publication 14 August 2024, date of current version 27 August 2024.

Digital Object Identifier 10.1109/ACCESS.2024.3443462

RESEARCH ARTICLE

Fabrication and Broadband Dielectric Study of Properties of Nanocomposites Materials Based on Polyurethane

ŠTEFAN HARDOŇ[1], JOZEF KÚDELČÍK[1], ANTON BARAN[2], PAVEL TRNKA[3] (Senior Member, IEEE), ONDREJ MICHAL[3] (Member, IEEE), ADAM TAMUS[4] (Member, IEEE), TOMASZ KOLTUNOWICZ[5], ALENA KOZÁKOVÁ[6], TOMÁŠ DÉRER[6], AND JAROSLAV HORNAK[3] (Senior Member, IEEE)

[1]Department of Physics, Faculty of Electrical Engineering and Information Technology, University of Žilina, Žilina 8215/1, Slovakia
[2]Department of Physics, Faculty of Electrical Engineering and Informatics, Technical University of Košice, 040 01 Košice, Slovakia
[3]Department of Technologies and Measurement, Faculty of Electrical Engineering, University of West Bohemia, 301 00 Pilsen, Czech Republic
[4]Department of Electric Power Engineering, Faculty of Electrical Engineering and Informatics, Budapest University of Technology and Economics, 1111 Budapest, Hungary
[5]Department of Electrical Devices and High Voltage Technology, Faculty of Electrical Engineering and Computer Science, Lublin University of Technology, 20-618 Lublin, Poland
[6]VUKI a. s., Electroinsulating resins and varnishes, 831 07 Bratislava, Slovakia

Corresponding author: Štefan Hardoň (stefan.hardon@uniza.sk)

This work was supported in part by the Grant System of University of Žilina under Grant 1/2023 (18735); in part by the Student Grant Agency of the University of West Bohemia in Pilsen "Materials and Technologies for Electrical Engineering" under Grant SGS-2024-008; in part by Slovak Research and Development Agency under Contract APVV-21-0078 and Contract APVV-21-0449; and in part by the Ministry of Science and Higher Education (Poland) for the Lublin University of Technology for Activities in Scientific Discypline Automation, Electronics, Electrical Engineering, and Space Technology under Grant FD-20/EE-2/703.

ABSTRACT The aim of study is addressing the influence of nanoparticles (NPs) on the dielectric properties of polyurethane. In this research, only investigated the effect of Al_2O_3, MgO and ZnO NPs for concentrations up to 2 wt.% with the temperature range from 25 to 120 °C. During the preparation of nanocomposites, polymer chains bind to NPs, which then limits their mobility. This effect results in a decrease in real permittivity and the course of polarization mechanisms. An increase in permittivity over the entire temperature range only for a 2 wt.% MgO concentration was observed. The decrease in the mobility of polymer chains was confirmed by dynamic-mechanical analysis. This method also results in an increase in the glass transition temperature depending on the type and concentration of NPs. The presence of NPs and the limited mobility of the polymer chains results in a shift of the low-frequency local maximum to lower frequencies.

INDEX TERMS Polyurethane, nanoparticles, dielectric spectroscopy, dielectric relaxation, DMA measurements.

I. INTRODUCTION

From the onset of the 21st century, there has been growing concern among scholars about nanocomposite materials. This fascination stems from the potential these materials hold for a wide array of applications. This is due to their exceptional and distinctive optical [1], dielectric [2], electrochemical [3], magnetic [4], mechanical properties [5] and biological [6], [7]. Furthermore, nanocomposite [8] insulation materials have many benefits. These include the absence of leaks, robust structural integrity, and thermal and electrical stability [9]. Moreover, they exhibit outstanding safety and compatibility with the life components of electric devices and battery electrodes [10].

Polyurethanes (PURs) represent a category of segmented copolymers comprising distinct soft and hard segments. The pliable segment typically consists of a polyether or polyester polyol, while the more rigid component consists

The associate editor coordinating the review of this manuscript and approving it for publication was Ajit Khosla.

of a diisocyanate and chain extender. Elasticity stems from the soft segment, whereas strength and rigidity arise from the hard segment, which forms physical cross-linking points [5], [11]. Over the past few decades, polyurethanes (PURs) have been extensively utilized across a wide range of applications. These include foams, polyurethanes [12], [13], elastomers [14], adhesives, paints, fibers (such as spandex), and specialized coatings for various purposes such as marine coatings, floor coatings, automotive coatings, aircraft coatings, pipeline coatings, industrial equipment coatings, medical device coatings, wood coatings, packaging coatings, and textile coatings [12], [13]. For each specific application, the chosen composition of polyurethanes confers essential physical traits tailored to the unique requirements of that application. Consequently, research concerning polyurethane has remained a prominent theme within polymer studies. Prior investigations have established that the interplay between structure and properties in polyurethanes is significantly influenced not only by the selection of initial materials but also by the polymerization technique, degree of phase separation, morphology, crystallization extent, and presence of hydrogen bonding within the final polymer. Recently, there has been a notable focus on modifying polyurethanes and evaluating their long-term reliability [15], [16].

It has been demonstrated that polymer blends, which are composed of a minimum of two distinct polymers, can be used to produce materials with desirable physical properties. One key benefit of polyurethanes is that, by making straightforward adjustments to the composition, a vast range of properties and characteristics can be achieved at an affordable cost. Additionally, the polymerization process typically takes place at ambient room temperatures. As a result of their versatility and value, these polymeric blends are widely used in a variety of industries. In practice, both foam polyurethane (hard, e.g., for thermal insulation in the construction industry, or soft for the production of mattresses or seat fillings) and compact PUR (without bubbles) are used, e.g., for the production of molded floors (and generally in the construction industry - composites), 3D printers [18], and as electrical insulation materials [10], [19], (encapsulation or waterproofing of transformers [4], [20], terminals, capacitors, fragile electrical circuits, car batteries [17], [21], etc.). A number of these characteristics include strong compatibility, favorable moldability, and the ability to adjust to meet specific performance and application requirements.

PUR characteristics can be enhanced through the utilization of nanoparticles, which possess distinctive qualities in various respects. NPs can bring about alterations in the physical and chemical attributes of the matrix. This primary impact is also associated with several fundamental phenomena, including their nanometer size [26], concentration [23], [24], active surface area, quantum size effects, and specific nature, among other factors [25].

Efforts to enhance PUR through nanoparticle modification, particularly focusing on alterations in dielectric properties, have been briefly outlined in existing literature. Notably, nanosilica [27], [28], [29], [30] and occasionally other oxides like ZnO [23], [32], [33], Al_2O_3 [3], [47] and TiO_2 [15], [24], $BaTiO_3$ [21], CeO_2 [5], or nitrides like BN [34], have been integrated into the pure resin. Consequently, the dielectric properties of the investigated nanocomposites are influenced by the nature of the polymer matrix and particle size, thier content, morphology, and particle size distribution of nanoparticles incorporated in a polymer matrix. The ongoing research and development in polymer nanocomposite materials open up novel prospects in nanotechnology, proving applicable to both industrial [35] and medical applications [36]. However, the primary objective of this study is to present fresh insights into the behavior of nanocomposite materials derived from a commercially utilized PUR containing dispersed nanoparticles of Al_2O_3, MgO and ZnO, across broadband frequency and temperature ranges. This exploration also encompasses additional findings from dynamic mechanical thermal analysis (DMA).

II. INVESTIGATED MATERIALS

The primary aim of this study is to elucidate the impact of incorporating filler materials such as magnesium oxide, zinc oxide, and aluminum oxide nanoparticles on both the dielectric characteristics and the structural attributes of a novel type of two-component PUR manufactured by VUKI a.s. under the name VUKOL N22 [37]. When considering the incorporation of nanoparticles as dopants in polymer matrices, it is imperative to address several critical parameters to achieve the desired enhancements in material properties. These parameters encompass particle size, surface modification, concentration of nanoparticles, dispersion, and the resultant effects on the polymer's mechanical, thermal, and electrical properties. The selection of nanofillers in this study is grounded in prior our research [23], [38], [39] which has demonstrated their efficacy in enhancing the insulating and dielectric properties of nanocomposites.

A. POLYURETHANE VUKOL N22

VUKOL N22, currently produced by VUKI a.s., under experimental examination, exhibits several distinctions from its precursor, VUKOL 022. Unlike VUKOL 022, which incorporates natural zeolite as a desiccant, VUKOL N22 utilizes synthetic zeolite powder in its production. Furthermore, VUKOL 022 lacked fire resistance, causing the PUR to ignite spontaneously upon exposure to flames. In contrast, VUKOL N22 has been enhanced with a liquid flame-retardant additive, allowing it to meet the V2/2 mm flammability class, according to the UL94 standard. This classification practically translates to a level of self-extinguishing capability. Moreover, there are disparities in the mechanical properties of these materials. VUKOL N22 includes additional crosslinkers, which facilitate the formation of a more densely crosslinked three-dimensional polymer structure during the curing process. As a consequence, the

newer PUR exhibits heightened mechanical strength and hardness, measuring at 77-80 Shore A. Additionally, its low initial viscosity makes it suitable for filling extremely narrow gaps or cavities, primarily within the realm of electrical insulation applications. This research presents an exceptional and comprehensive investigation into the formulation and analysis of nanocomposite materials from both a preparation and dielectric perspective [40].The outcomes offer valuable insights, particularly for customizing material properties to suit diverse applications, extending beyond the realm of high-voltage technology.

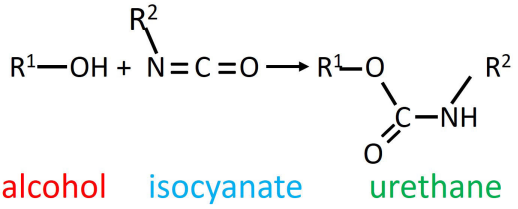

FIGURE 1. Polyurethanes are synthesized by reacting isocyanate groups in the hardener molecule with hydroxyl groups in the polyol. [41].

Investigated PUR is a two-component (2C) polyurethane potting compound with low initial viscosity, room temperature curing, low solid filler content, and is solvent free (volatile organic compounds < 1%). After curing, it resembles hard rubber and belongs to the class of medium-hard PURs. The studied PUR is suitable for potting or encapsulating electrical equipment such as small or medium transformers, capacitors, coils, electronics, and car batteries. Due to its high ductility, it is suitable for potting materials with different coefficients of thermal expansion. Free of abrasive fillers, it is particularly suitable for continuous machining. Due to the low initial viscosity of the mixture, it can also be used for filling very narrow gaps or cavities. The temperature resistance of this type of potting compound ranged from − 40 °C to + 150 °C.

For 2-component (2C) systems, the initial element denoted as A represents an organic polyol (a polyunsaturated alcohol, usually with various additives), while the subsequent element denoted as B stands for a hardener derived from isocyanate. From a chemical standpoint, the fundamental curing process involves the additive reaction between the isocyanate groups within the hardener compound and the hydroxyl groups present in the polyol compound. This reaction follows a general equation, as illustrated in Fig. 1. The polyol also comprises some solid additives (in a finely powdered form), which tend to sediment over time. Prior to combining the A and B elements of the 2C system, it is imperative to diligently blend and make the polyol component (element A) uniform. This step ensures the dispersion of any sediment throughout the volume. Subsequently, the hardener is introduced (its quantity determined by the mixing ratio, a parameter that should be adhered to with high precision). Following this, the entire reactive mixture undergoes a thorough homogenization process. A more detailed description of the polyurethane potting material is available [37].

TABLE 1. Parameters of nanopatricles: Magnesium Oxide, Zinc Oxide and Aluminium Oxide.

	MgO	ZnO	Al_2O_3
Purity (%)	> 99	> 99	> 99.97
Specific Surface Area (m^2/g)	60	40	180
shape	ellipsoidal or sperical	spherical	spherical
size (nm)	20	20	20-30
Color	white	white	white
Bulk Density (g/cm^3)	0.1 – 0.3	0.1 – 0.2	3.95
pH value	7.5 – 8.5	6.5 – 7.5	5.0 – 7.5

B. NANOPARTICLES

The final nanocomposites are composed of PUR blended with nanoparticles (NPs) having a spherical shape and an average particle size of 20 nm at concentrations of 0.5 wt.%, 1 wt.% and 2 wt.% by weight (further than %). Selecting the size of nanoparticles employed in these experiments of nanocomposites is a critical decision that influences the resulting material properties. or dielectric applications, nanoparticles should be small enough to disperse uniformly but large enough to prevent quantum size effects that might alter electrical properties [42]. The selected nanoparticles, aluminum oxide Al_2O_3 [43], magnesium oxide (MgO) [44] and zinc oxide (ZnO) [45] were chosen based on previous research [23], [38], [41], [46] demonstrating their ability to enhance the insulating and dielectric properties of the nanocomposite materials under investigation. The fundamental characteristics of the nanoparticles employed are detailed in Table 1 [43], [44], [45]. As a result of the outcomes from their experiments, these nanocomposites containing these nanoparticles have been tailored to meet the stringent insulation standards needed by high-voltage power equipment. This adaptation aligns with the increasing needs stemming from the growing generation and consumption of power.

Magnesium oxide, also known as magnesia or MgO, garners significant attention for its remarkable attributes, including non-toxicity, high thermal conductivity and stability, low dielectric constant, exceptional corrosion resistance, and a high modulus of rupture. It finds applications across various industries such as wastewater treatment, ceramic protection, optoelectronic materials, and as a fire retardant. MgO, widely available as an alkaline earth material, is environmentally benign, serving as an insulator with a band gap: $E_g = 7.8$ eV [41] and a notable relative permittivity 9.9 [22].

The distinctive chemical properties and expansive surface area of nanostructured MgO have expanded its usage in diverse contemporary applications. In the medical realm, MgO contributes to cancer treatment, exhibits antibacterial properties, and aids in bone regeneration. Furthermore, MgO nanoparticles (NPs) synthesized via sol-gel and flame spray pyrolysis techniques have demonstrated remarkable efficacy

in textile applications and the removal of methylene blue dye [6].

In recent years, zinc oxide nanoparticles have garnered increasing attention owing to their distinct physical and chemical characteristics. These nanoparticles not only demonstrate thermal stability but also boast appealing antibacterial properties. Additionally, they are pose relatively minimal risk to the environment. Incorporating zinc oxide nanoparticles into polymers has shown notable benefits, enhancing their properties for tasks like pollutant adsorption or catalytic degradation. Moreover, this integration amplifies their antibacterial efficacy, offering a multifaceted approach to environmental and health-related challenges [23], [24], [32], [33], [46].

Alumina nanoparticles Al_2O_3 are garnering increasing attention across various industries due to their exceptional properties and versatile applications. These nanoparticles, composed of aluminum oxide, exhibit remarkable mechanical strength, high thermal conductivity, and excellent chemical stability. With a wide bandgap and electrical insulation properties, alumina nanoparticles are utilized in various fields, including electronics, ceramics, catalysis, and biomedical applications. In electronics, alumina nanoparticles serve as essential components in the fabrication of insulating layers, interconnects, and dielectric materials due to their excellent electrical insulation properties and high thermal conductivity. In the ceramics industry, alumina nanoparticles are utilized to enhance the mechanical strength, hardness, and wear resistance of ceramic materials. Their incorporation into ceramic composites improves their structural integrity and thermal stability, making them ideal for high-temperature applications such as cutting tools, wear-resistant coatings, and refractory materials. Furthermore, in biomedical applications, alumina nanoparticles find use in drug delivery systems, bioimaging, tissue engineering, and medical diagnostics. Their biocompatibility, low toxicity, and surface functionalization capabilities make them suitable for targeted drug delivery and imaging contrast agents, as well as scaffolds for tissue regeneration [46], [47], [48].

III. TECHNOLOGICAL PROCEDURE OF NANOCOMPOSITE SAMPLES PREPARATION AND MEASUREMENT TECHNIQUES

A. TECHNOLOGICAL PROCEDURE OF NANOCOMPOSITE SAMPLES PREPARATION

As mentioned in our previous studies [23], [38], [41], [46], in the preparation of nanocomposite dielectric materials using a PUR potting compound matrix enhanced with nanofillers, there are two fundamental mixing mechanisms. The first method described earlier involves a straightforward mixing process, wherein the initial components' particles are randomly dispersed in the mixture without altering their physical characteristics, mingling with other random particles. The second mechanism in this process is dispersive mixing, which aims to reduce the clustering of solid particles within the liquid polymer. This is carried out to ensure their even distribution throughout the polymer's volume.

Before mechanically blending the nanoparticles with the 2-component (2C) system, the individual nanoparticles underwent a 24-hour drying process in a laboratory vacuum hot air dryer at a temperature of 40 °C and standard laboratory air pressure to eliminate surface moisture. To achieve a more favorable viscosity for mechanical mixing, the component marked as A (organic polyol) was heated to 40 °C. To create the necessary weight concentrations for the nanocomposite samples (0.5, 1.0, and 2.0 %), it was essential to precisely determine the weight of the dried NPs before adding them to component A's matrix. Subsequently, the matrix of component A and the individual nanoparticles were mechanically mixed for a duration of 5 hours at 40 °C using a magnetic stirrer (500 rpm) in a laboratory vacuum dryer. This was followed by additional mechanical mixing involving an ultrasonic needle for 1 hour. The next step was a vacuuming process for 3 hours at a pressure of 10 mbar with the magnetic stirrer running at 500 rpm. The purpose of the vacuuming process is to eliminate all air bubbles from the prepared suspension. NPs employed in nanocomposite dielectric materials exhibit strong cohesive forces. A critical factor that impacts the characteristics of the ultimate nanocomposite material is the accurate dispersion of these NPs. It is conceivable that aggregate formation could not only diminish the overall dielectric properties but also potentially affect space charge phenomena. Thus, to prevent agglomeration, the ultrasonic needle appears to be a very useful laboratory tool [26], [49], [50], [51]. Then, the hardener (marked as element B) was added to the mixture at the recommended ratio (100:47) [37]. Utilizing this approach ensures the even distribution of the nanofillers within the liquid polymer matrix, even when the nanoparticle concentrations are extremely low. TThe completed suspension mixture (consisting of element A, element B, and nanoparticles) was poured into flat, circular molds with a diameter of 90 mm and a final sample thickness of 1.5 mm. The last step marked as Sample finishing includes identification of produced samples by special pen marker. Each set of prepared samples included five samples, each with a particular nanoparticle concentration, to ensure that the measured results could be replicated and verified. The processes for creating the investigated nanocomposites are illustrated in Fig. 2.

Only SEM photos and photos of the prepared samples (PUR + MgO) are shown in Fig. 3 because, for other types of nanocomposite samples with Al_2O_3 and ZnO nanoparticles the photos are very similar. To verify particle dispersion, a Phenom ProX desktop SEM microscope (Thermo Fisher Scientific, Breda, The Netherlands) was equipped with a backscattered electron detector. With an applied acceleration voltage of 15 kV, observations were conducted in low vacuum and charge reduction mode. An almost homogeneous distribution of nanoparticles can be seen from the surface analysis. In the photos of the samples, there is pure PUR and

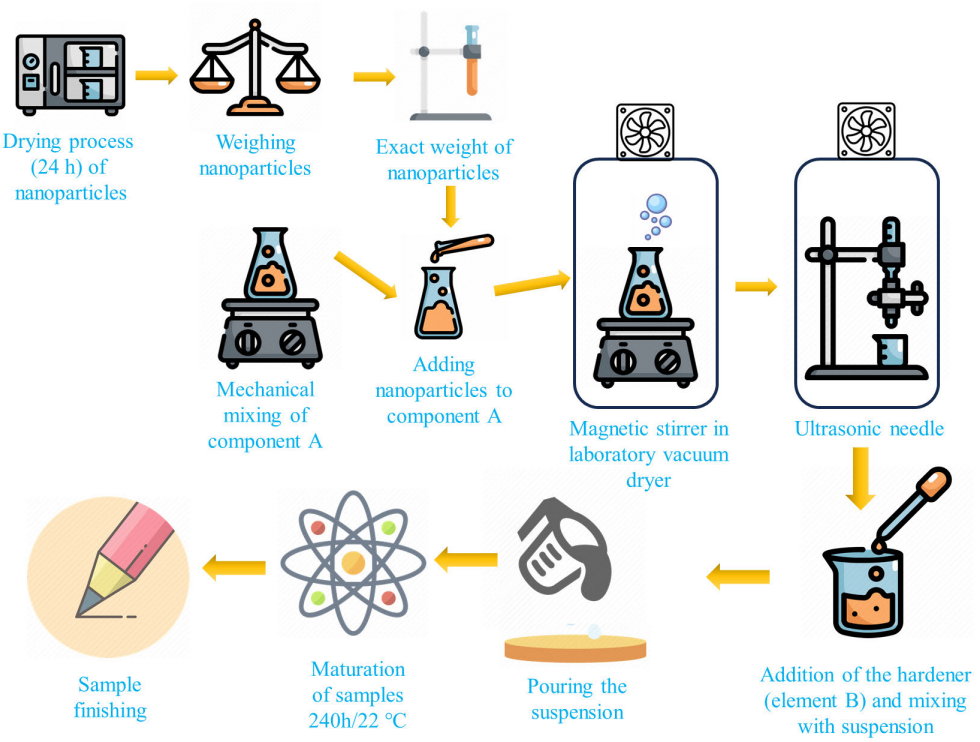

FIGURE 2. Technological procedures in the preparation of nanocomposites.

then successively the results of the nanocomposite with 0.5, 1.0 and 2.0 wt % MgO.

A polymer is composed of chains, structures, and other segments with various charges, which produce permanent or induced dipoles when placed in an electric field. With the motion of dipoles in the AC electric field, a variety of processes are connected, such as interfacial polarization (IP) relaxation γ, β and α- relaxations, the Maxwell-Wagner-Sillars (*MWS*) effect, the intermediate dipolar effect (*IDE*) and DC conductivity [48], [51], [52]. The motion of phenyl rings and C-H units is related to the fastest γ - relaxation at low temperatures (low thermal energy). The rotation of polar groups around C-C bonds or the mobility of the side groups of a polymer are the main parts of β - relaxation [24], [52], [53], [54]. IDE relaxation is associated with the local motion of chain segments of the polar side groups around the C-C bond. This is most likely attributed to the motion of the polar carbonyl groups that form the structural base of PUR [55], [56]. α- Relaxation relates to the glass transition temperature T_g and occurs due to microscale Brownian motion, and DC conductivity overshadows this relaxation at low frequencies. These mechanisms were observed in TiO_2 or ZnO resin microcomposites [24], [53], [54].

B. MEASUREMENT TECHNIQUES

Dynamic-mechanical analysis (DMA) was performed on a DMA Q800 (TA Instruments, New Castle, DE, USA) analyzer with the gas cooling accessory (GCA) filled

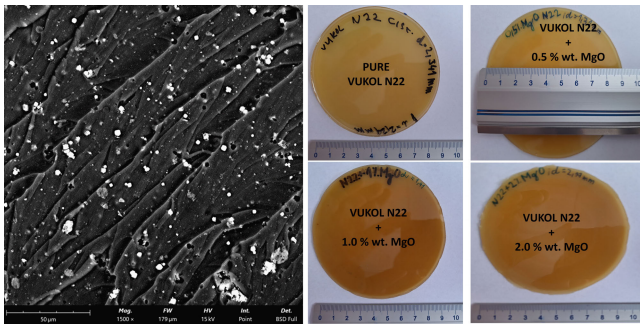

FIGURE 3. Particle dispersion analysis of PUR doped with 2.0 wt % MgO (left) and color change of the investigated PUR composites with different concentrations of MgO with a real scale in cm (right).

with liquid nitrogen to provide sub-ambient temperatures. The dual cantilever operational mode was used for all experiments, and the sample length between the clamps was approximately 13 mm. The sample was cooled quickly to - 60 °C and maintained at this temperature for 3 min. Consequently, the samples were heated to 90 °C at a heating rate of 3 °C/*min* in a nitrogen atmosphere while displacement with a frequency of 1 Hz and amplitude of 5 μm was applied.

The capacitance method was employed to assess both the real and imaginary components of complex permittivity across a frequency spectrum spanning from 1 mHz to 1 MHz. Measurement of these parameters was carried out using a precision LCR meter, specifically the QuadTech 7600+,

covering frequencies from 100 Hz to 1 MHz, and the IDAX 350 for frequencies from 1 mHz to 10 kHz. Testing of a flat circular sample (diameter 90 mm, thickness 1.5 mm) across temperatures ranging from +20 °C to +120 °C was conducted using a controlled oven, with measurements facilitated by a three-electrode system. Additionally, the impact of temperature on the real capacitance and tangent loss factor was examined using the 50 Hz Tettex 2840 High Precision C and Tan D Measurement Bridge. The Alpha-A measuring instrument, manufactured by Novocontrol Technologies in Montabaur, Germany, equipped with the essential ZGS electrode system, was employed for conducting validation measurements.

TABLE 2. Glass transition temperatures (°C) estimated as the peak maxima of the tan δ curves for pure PUR and its nanocomposites with different weight concentration (wt.%) of various nanoparticles.

NPs	MgO	ZnO	Al_2O_3
wt.%	^oC	^oC	^oC
0	34.6	34.6	34.6
0.5	35.4	48.5	36.6
1.0	33.2	42.2	50.3
2.0	35.4	43.2	36.5

IV. EXPERIMENTAL RESULTS

A. DYNAMIC-MECHANICAL ANALYSIS

As for DMA experiment, a harmonic force of constant frequency is applied to the studied sample at a given temperature, and the mechanical response to this force is measured. The storage modulus, loss modulus and mechanical damping factor are the main characteristics obtained from DMA experiments. The storage modulus represents the energy stored in the system, the loss modulus measures the dissipated energy in one cycle of deformation, and the ratio of loss and storage moduli is called the mechanical damping factor tan δ. The temperature associated with the peak magnitude of the tan δ. temperature dependence of polymers is usually defined as the glass transition temperature T_g. The T_g is a temperature at which polymer chains in amorphous regions of a polymer undergo a relaxation transition from a rigid structure to a rubbery state. In addition to information concerning the glass transition temperature, the intensity of molecular motion can also be deduced from the results of DMA measurements. The shift of the glass transition temperature to higher values usually reflects the reduced mobility of chains present in the amorphous phase of the polymer and vice versa.

The temperature dependence of tan δ in the range of −60 °C to 90 °C for pure PUR and its nanocomposites with Al_2O_3 NPs is shown in Fig. 4a). The values of the glass transition temperature T_g (peak of tan δ in temperature dependence) are listed in Table 2. For all nanocomposites containing Al_2O_3, the T_g shift to higher values was observed, which reveals a decrease in the segmental motion of polymer chains due to the presence of nanoparticles in the polymer matrix. This effect is more pronounced for the composite with 1 wt.% of Al_2O_3, probably as a result of the uniform dispersion of nanoparticles in the polymer matrix.

The influences of different types of nanoparticles on the relaxation transition of PUR were also studied, and the tan δ temperature dependences for composites with various wt.% of Al_2O_3, ZnO and MgO are depicted in Fig. 4. As seen from Fig. 4d), mixing MgO and Al_2O_3 nanoparticles to PUR only slightly increased the T_g values in contrast to ZnO NPs, where an increase in T_g of 10 °C compared to pure PUR was observed. Lower polymer chain mobility in all nanocomposites can be deduced from the increase in the T_g value. This effect is most pronounced for the ZnO NPs nanocomposites and could be explained by a stronger interaction between the polymer matrix and the ZnO NPs than in the case of Al_2O_3 and MgO NPs.

B. FREQUENCY DIELECTRIC SPECTROSCOPY

1) THEORETICAL ANALYSIS OF THE INFLUENCE OF POLARIZATIONS ON COMPLEX PERMITTIVITY

The complex permittivity, often denoted as $\varepsilon^*(\omega)$, is a property of materials that describes their ability to respond to an applied electric field at different frequencies. It is a complex number because it has a real part (ε') and an imaginary part (ε'') of the complex part. ε'' indicates the dielectric losses, occurring after an impact of AC, of factors such as conductivity, various polarizations, and other factors. The tangent loss factor (dissipation factor or simply as the loss tangent) denoted as tg $\delta = \varepsilon''/\varepsilon'$, is a measure of the energy loss in a dielectric material when it is subjected to an alternating electric field, and it shows the lack of efficiency in polarizing a material.

In weakly polar liquid dielectrics, the complex permittivity is described through the Debye equation [58], [59] with one relaxation time (τ_0) or a eigenfrequency $f_0 = 1/(2\pi\tau_0)$. The complex permittivity in polymers is influenced by more factors, such as dipole molecules orientation in external field, a magnitude of a electric filed, what result in varying relaxation times (τ_{0i}). For this case is better used the Cole-Cole distribution [60], while the effects of the interface between the NPs and the polymer matrix must also be considered. In addition to the polarization processes taking place in a real dielectric, there are also the conductivity losses due to oscillating of free charge carriers near electrodes and in polymer matrix with NPs. The complex permittivity with losses by DC conductivity (σ_{DC}) [46], [60] has the following form:

$$\varepsilon^* = \varepsilon_\infty + \frac{\Delta\varepsilon_1}{1+(j\omega\tau_1)^{1-a_1}} + \frac{\Delta\varepsilon_2}{1+(j\omega\tau_2)^{1-a_2}} - j\frac{\sigma_{DC}}{\varepsilon_0\omega} \quad (1)$$

where ε_∞ is "infinite frequency" dielectric constants, $\Delta\varepsilon_i$ is the change of real part of complex permitivity, a_i is the distribution parameter ($0 \leq a \leq 1$). Dielectric relaxation can also be modeled by several other empirical functions (Cole-Davidson or Havriliak-Negami [61], [62], [64]).

An illustration of the impact of two polarization processes and conduction losses on the complex permittivity in the

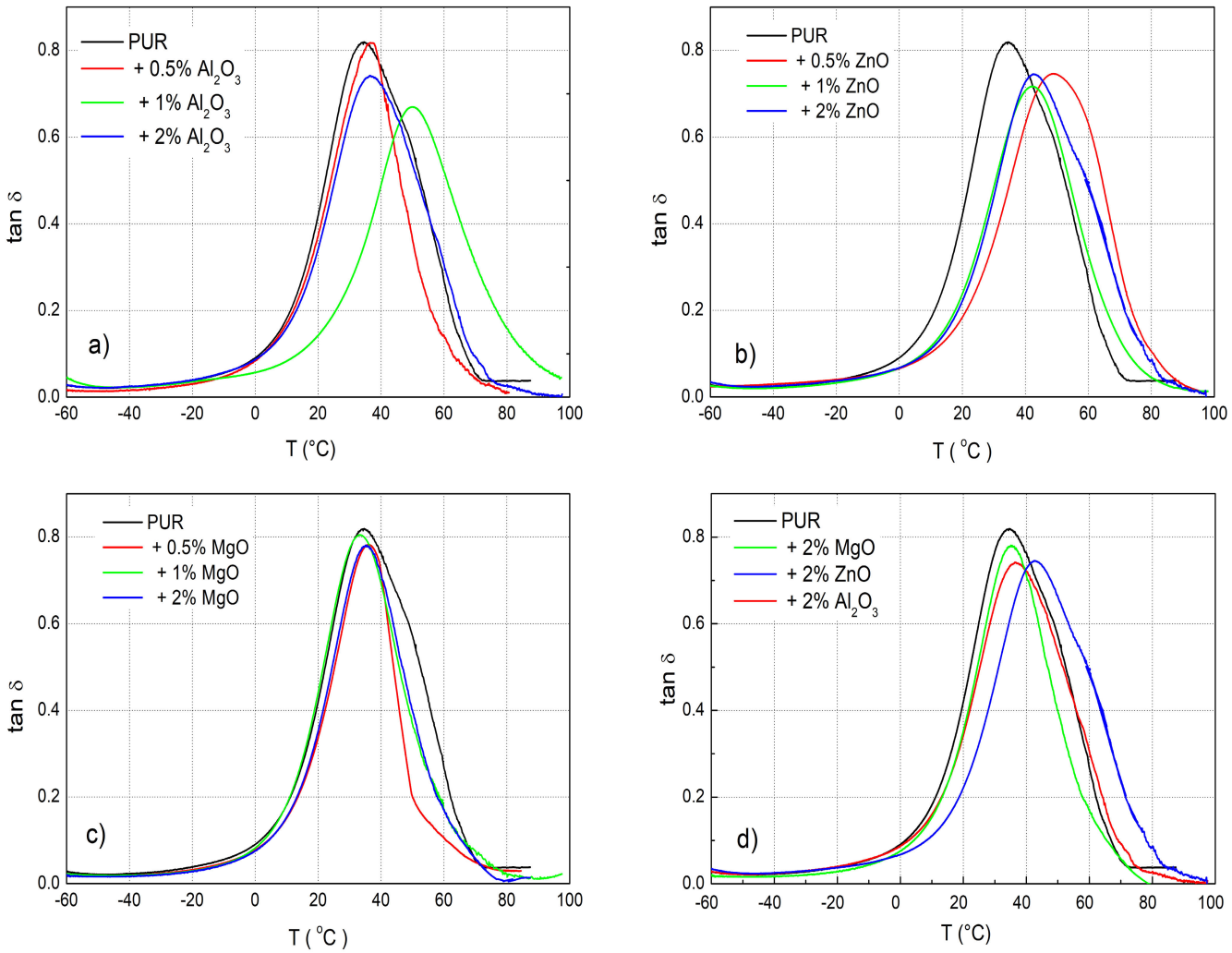

FIGURE 4. Temperature dependence's of the mechanical damping factor tan δ measured for pure PUR and its nanocomposites containing 0.5 wt.%, 1 wt.% and 2 wt.% of a) Al_2O_3, b) MgO and c) ZnO. d) Curves of the mechanical damping factor tan δ for composites with 2 wt.% of Al_2O_3, ZnO and MgO nanoparticles.

double logarithmic coordinates is presented in Fig. 5. For drawing this frequency development, the Cole-Cole model with data from Table 3 for temperature at 60 °C was used. Real part of complex permittivity (Fig. 5a) for frequency below 2 mHz reaching maximum permittivity ε_s (the same as for the static electric fields). With increasing frequency, the real permittivity (green curve) begins to gradually decrease, what relates to polarization process at eigenfrequency $f_2 = 6$ mHz (dark yellow curve). At eigenfrequency $f_1 = 718$ Hz influence on the real permittivity the next polarization process (purple curve). Furthermore, in case of higher frequencies, the real permittivity decreases exponentially asymptotic to the lowest theoretical value ε_∞. High values of the imaginary part of complex permittivity (Fig. 5b) at very low frequencies is mainly caused by the conduction losses (blue curve). The local maxima at eigenfrequencies (f_1, f_2) caused by two polarization processes are more pronounced. The process occurs at low frequencies (dark yellow curve) has sharp maximum, related to the small value of the a_2 coefficient and the relaxation processes at eigenfrequency f_1 (purple curve) is in a wider range of frequencies.

C. INFLUENCE OF NANOPARTICLES ON THE COMPLEX PERMITTIVITY

Frequency dependence's of the complex permittivity of PUR with 2 wt.% of Al_2O_3 NPs for different temperatures (25 °C $\leq$ T $\leq$ 120 °C) are shown in Fig. 6. As the temperature increases, we observe that the complex permittivity curves shift from a lower to a higher frequency. The real part of the complex permittivity (ε' or real permitivity) at a temperature of 25 °C changes only slightly (Fig. 6a); it increases almost linearly from 3.8 (1 MHz) to 8 (1 mHz). With an increase in temperature in the subhertz frequency range, is observe a gradual increase up to 30 at a temperature of 60 °C. This increase was caused by an electrode polarization-type effect, which can arising from the agglomeration of

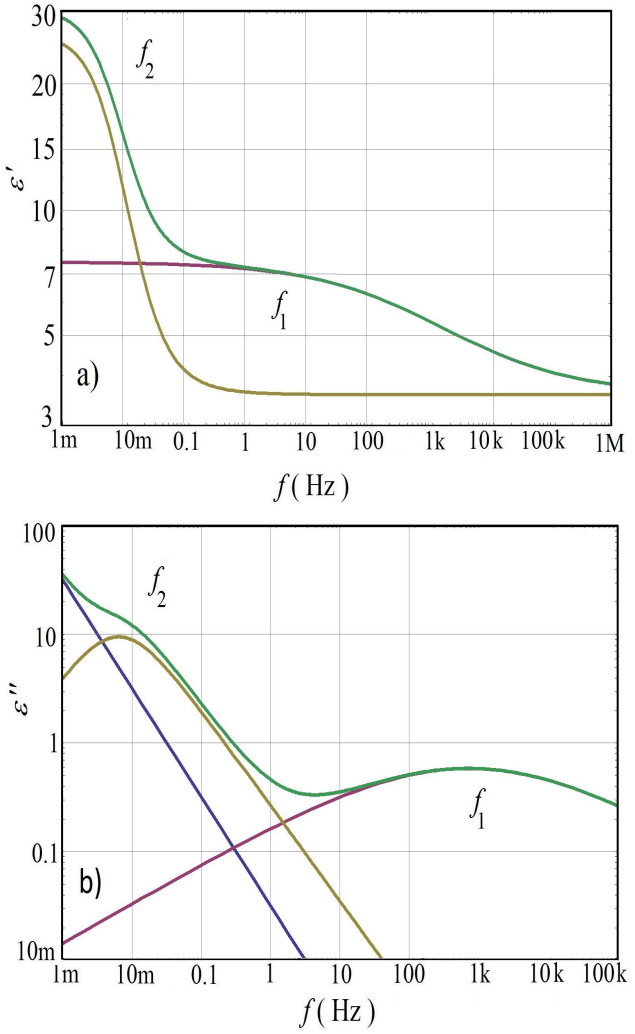

FIGURE 5. Frequency dependence of the real (a) and imaginary (b) part of complex permitivity with two polarization processes and dc conductivity losses drawn by Cole-Cole model (1) ($\varepsilon_S = 17.3$, $\varepsilon_\infty = 3.6$, $f_{01} = 718$ Hz, $a_1 = 0.63$, $f_{02} = 6$ mHz, $a_2 = 0.12$, $\sigma_{DC} = 1.9 \times 10^{-12}$ S/m).

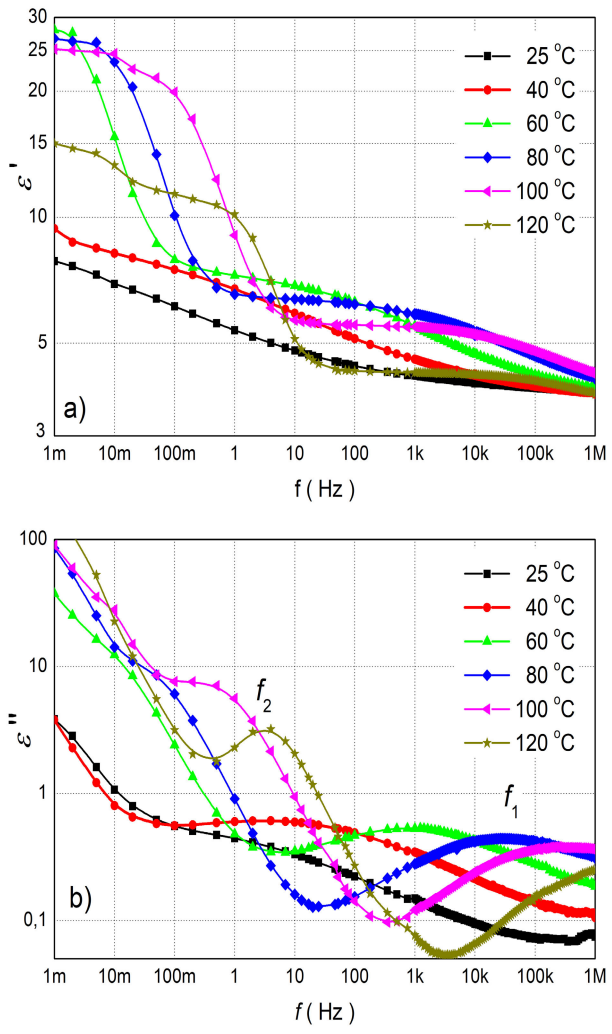

FIGURE 6. The frequency dependence of the real part of (a) and (b) imaginary part of the complex relative permittivity for PUR with 2 wt.% Al_2O_3 nanoparticles.

charge carriers at the interface between the sample under investigation and the electrodes [63]. For a temperature of 60 °C and higher a significant decrease in ε' between 10 mHz and 10 Hz is observe. In the case of higher frequencies than 1 kHz, a local maximum is also less pronounced. The development for the imaginary part of the complex permittivity (ε'') (Fig. 6b) is approximately the same with two main different features. First, the imaginary part of the complex permittivity at subhertz frequencies reaches significantly higher values, and second, two local maxima (f_1, f_2) are more visible. With an increase in temperature, their positions shifted to higher frequencies. Nanocomposites are complex systems containing polymer chains, nanoparticles, connections between them through interphase layers and other parts or processes. On this basis, to determine the parameters of the relaxation processes and the dielectric properties of the nanocomposite (Table 3), the Cole-Cole model (Eq. (1)) was used, which is widely used by other authors [57], [65], [66].

A comparison of ε' and tg δ at 60 °C for pure PUR and nanocomposites with different Al_2O_3, MgO and ZnO concentrations are shown in Fig. 7. The temperature of 60 °C is interesting mainly for application purposes, as it is often the working temperature of rotating and non-rotating machines in electrical engineering area. For frequencies above 1 Hz, ε' (Fig. 7a) of Al_2O_3 and (Fig. 7e) ZnO nanocomposite samples was smaller than that of pure PUR [13, 43]. Only for 2 wt.% MgO was observed an increase of ε'. In the case of the all wt.% nanoparticles we observed the most significant decrease in the nanocomposite's permittivity between 1 Hz to 100 kHz. This relates to the biggest decrease in the segmental motion of polymer chains. Generally, at frequencies below 100 mHz, the effect of concentration is not as clear as it was at higher frequencies. The influence of different nanocomposites only at the frequency of 50 Hz as a function of temperature is

TABLE 3. Parameters of the Cole-Cole model for PUR with 2 wt.% Al_2O_3 at various temperatures, where ε_∞ is the high-frequency limit of the permittivity, σ_{DC} (10^{-12} S/m) is the DC conductivity, τ is the relaxation time, $f_0 i = 1/(2\pi\tau)$ and a is the shape parameter.

T(°C)	40	60	80	100	120
ε_∞	3.3	3.6	3.6	3.7	3.2
σ_{DC}	0.9	1.9	5.8	15	15.2
$\Delta\varepsilon_1$	0.3	3.9	2.8	1.7	1.1
$f_{02}(Hz)$	0.54	718	3.25k	185k	1.44M
τ_1 (s)	0.29	0.22m	4.9μ	4.9μ	0.11μ
a_1	0.6	0.63	0.62	0.48	0.48
$\Delta\varepsilon_2$		23.1	20.3	17.5	7.1
f_{02} (mHz)		6m	34m	346m	3.1
τ_2 (s)		24.8	4.62	0.46	0.05
a_2		0.12	0.16	0.17	0.08

demonstrated in Fig. 9. The different concentrations caused a shift in the local maxima of the tg δ (tangent loss factor) (Fig. 7b,d,e), what could relate to measurement of the mechanical damping factor tan δ (Fig. 4a). In case of the 2 wt.% Al_2O_3 and MgO and all wt.% ZnO, the α-process shifted to a lower eigenfrequency f_{02} (Table 4), while only 0.5 and 1.0 wt.% MgO was shift opposite. There was minimal change of the other maxima of tg δ for all wt.% NPs to pure PUR. 0.5 wt.% Al_2O_3 shifted maxima to higher frequence's, smaller values of tg δ at 60 °C. At the 1 wt.% Al_2O_3, 0.5 and 1.0 wt.% ZnO there was only a shift in the IDE relaxation process to a lower eigenfrequency f_{01} (Table 4), what relates to a decrease in the mobility of segmental parts of the polymer chain in the free space around the NPs. All Cole-Cole parameters of the complex permittivity at studied concentrations only for temperature 60 °C are listed in Table 4.

We also studied the effect of other nanoparticles, MgO and ZnO, on complex permittivity in our experiments. From the measured temperature-frequency dependence's of the complex permittivity, a similar conclusion of the influence of NPs as was observed for Al_2O_3 emerged. There were changes in permittivity and a shift in the infrequence's of the α and *IDE* relaxation processes dependent on the temperature and concentration. At temperature 60 °C and in case of ZnO NPs small decrease of real permitivity with concentration at frequencies above 1 Hz was observed (Fig. 7e). Its lower values relate to decrease of polymer chain mobility - shift of tan δ to higher temperature (Fig. 4b), higher T_g values for all studied concentrations (Table 2) except for the 2 wt.% MgO. Admixture of MgO caused bigger changes on the real permitivity of nanocomposite. At the 0.5 wt.% and 1 wt.% a decrease of real permitivity at frequencies above 1 Hz was observed (Fig. 7c), as for Al_2O_3 and ZnO NPs. The 2 wt.% however, it causes an increase in real permittivity compared to pure PUR. This effect is associated with its high real permittivity of 7.8 and higher polymer chain mobility, smaller values of tan δ at 60 °C (Fig. 4b).

For comparison of the effect of 2 wt.% of different NPs on the real permittivity and tangent loss factor, was selected a temperature of 60 °C (Fig. 8). The DMA measurements (Fig. 4) showed that at 80 °C and higher, the polymer chains already had a large degree of freedom, and the difference between the effects of different NPs was minimal. This effect was mainly due to strong thermal motions that disturb the orientation of the individual dipoles in the material structure [54]. The 0.5 wt.% and 1 wt.% of all studied NPs caused a decrease or a small change in permittivity compared to pure PUR (Fig. 7a,c,d). In Fig. 8, the influences of different of NPs on the real permittivity can be clearly seen. For MgO, an increase is observed, and for Al_2O_3 and ZnO, we observed a decrease with respect to pure PUR.

The change in real permittivity only at the frequency of 50 Hz measured by Tettex 2840 but in the whole measured temperature range is shown in Fig. 9. Pure PUR real permittivity in the given temperature range changed between 4.7 and 7, with a maximum at 60 °C. For all NPs with 0.5 and 1 wt.% in PUR at temperatures below 80 °C (Fig. 9a, b) and 2 wt.% Al_2O_3 and ZnO at temperatures below 70 °C (Fig. 9c) the real permitivity was smaller, what was caused by low concentration and mainly lower polymer chain mobility, higher T_g values (Table 2). For all measured temperatures of 2 wt.%. MgO, there was an increase in real permittivity to pure PUR (Fig. 9c). This increase is caused with its high real permittivity of 7.8 and higher polymer chain mobility, smaller values of tan δ at 60 °C (Fig. 4c). The decrease in the case of all wt.% NPs at temperatures over 70 °C was also associated with a more significant shift of tg δ to higher temperatures. The increase at a temperature of 120 °C for 2 wt.% ZnO was influenced by the strong influence of the α-process, the local maximum of which at the given temperature was at 80 Hz.

V. DISCUSSION

Nanoparticles have a significant impact on the dielectric properties (complex permittivity and tangent loss factor) of PUR. The dynamic-mechanical analysis and the dielectric frequency spectroscopy (DFS) were used to identify the influence of NPs on the mobility of polymer chains and polarization processes in nanocomposite materials. These processes are temperature dependent, so measurements were also performed at different temperatures. In all studied nanocomposites, the T_g values increased, and polymer chain segmental motion decreased due to NPs present in the matrix. Realized experiments show that NPs have an influence on the real permittivity of polyurethane at 50 Hz (Fig. 9) as well as in a wider frequency range (Figs. 7, 8).

The real permittivity of nanocomposites is affected by NPs and polymer chain, which is bound to them. The binding of polymer chains to heavy NPs is associated with a decrease in their mobility. The change in the mobility of the polymer chains was confirmed by DMA measurements, where T_g (Table 2) shift to higher values corresponds to a decrease in the segmental motion of polymer chains due to the presence of nanoparticles in the polymer matrix. The mobility of chains and their arrangement in layers around NPs can be explained using three layers of Tanaka's model [57], [65]. They were

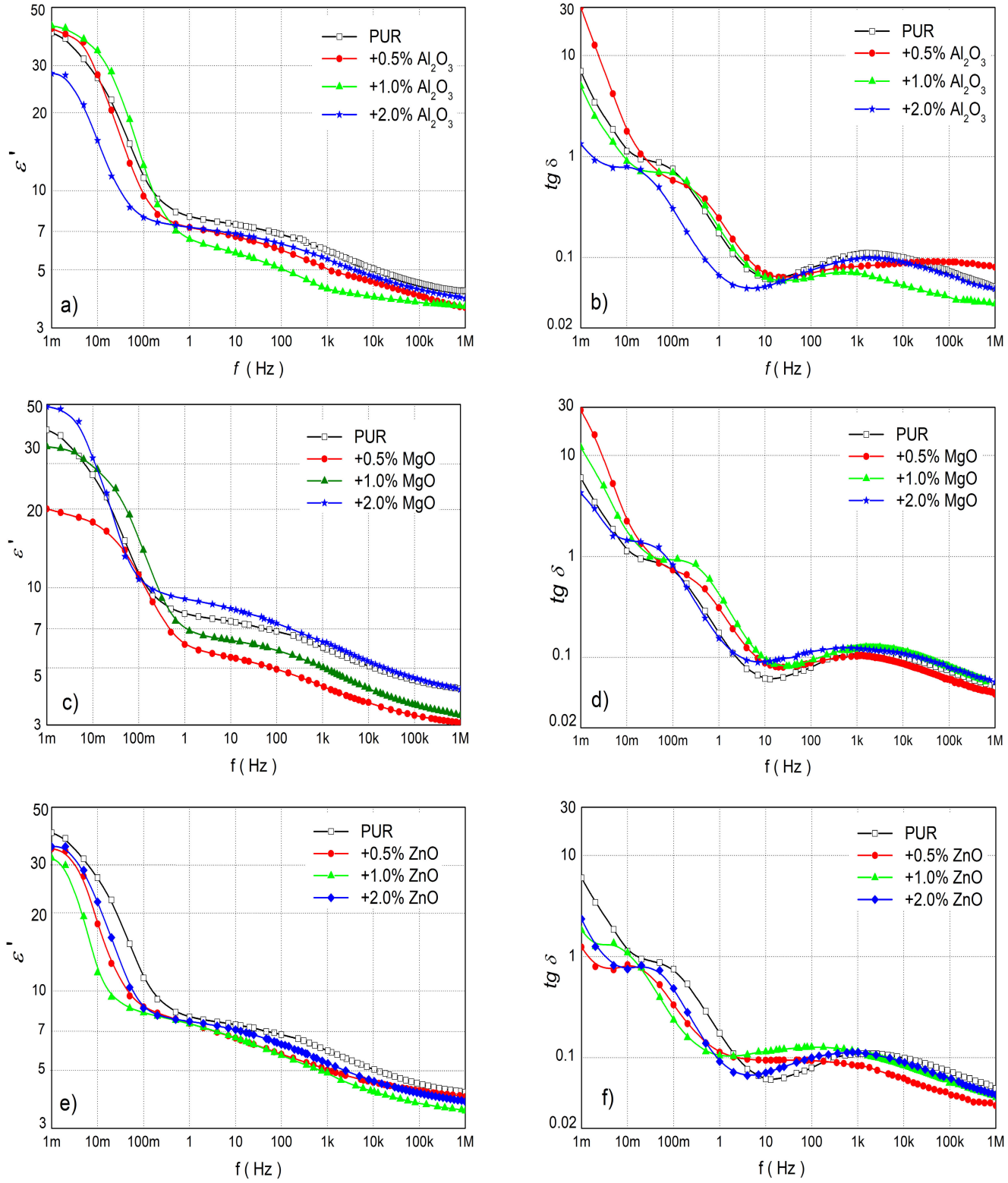

FIGURE 7. The frequency dependence of the real part of the complex relative permittivity and tangent loss factor for PUR with various concentrations of Al_2O_3 (a, b) MgO (c,d) and ZnO (e, f) nanoparticles at temperature 60 °C.

the significant reduction of the polymer chain mobility and dipoles in bounded and bound layers, which are the closest to the surface of the NPs [43, 47, 60]. The mobility reduction in the outer or loose layer was a secondary effect. In the

TABLE 4. Parameters of the Cole-Cole model for PUR and its mixture with Al_2O_3 and 2 wt.% MgO and ZnO at 60 °.

Parameter	unit	PUR	+0.5 wt.% Al_2O_3	+1 wt.% Al_2O_3	+2 wt.% Al_2O_3	+0.5 wt.% % MgO	+1 wt.% % MgO	+2 wt.% % MgO	+0.5 wt.% % ZnO	+1 wt.% % ZnO	+2 wt.% % ZnO
ε_∞		3.9	3.8	3.64	3.6	2.8	3.1	3.6	3.7	3.0	3.7
σ_{DC}	10^{-12} S/m	14.2	28.4	12.6	1.9	25.2	44.4	1.9	2.16	3.23	16.1
$\Delta\varepsilon_1$		3.85	2.8	2.4	3.9	3.9	3.8	3.4	6.9	9.5	5.9
τ_1	μ s	128	25	820	220	930	72	220	1561	1249	350
f_{01}	Hz	1240	6370	193	718	170	2230	718	102	123	454
a_1		0.6	0.6	0.53	0.63	0.7	0.6	0.63	0.76	0.8	0.69
$\Delta\varepsilon_2$		25.6	15.9	36.6	23.1	10.1	24.3	23.1	26.7	26.0	48.3
τ_2	s	3.67	2.47	6.06	24.8	1.29	1.37	24.8	23.5	43.3	15.9
f_{2e}	mHz	25	64	26	6	123	117	6	7	4	10
a_2		0.21	0.03	0.26	0.12	0.04	0.13	0.12	0.05	0.05	0.11

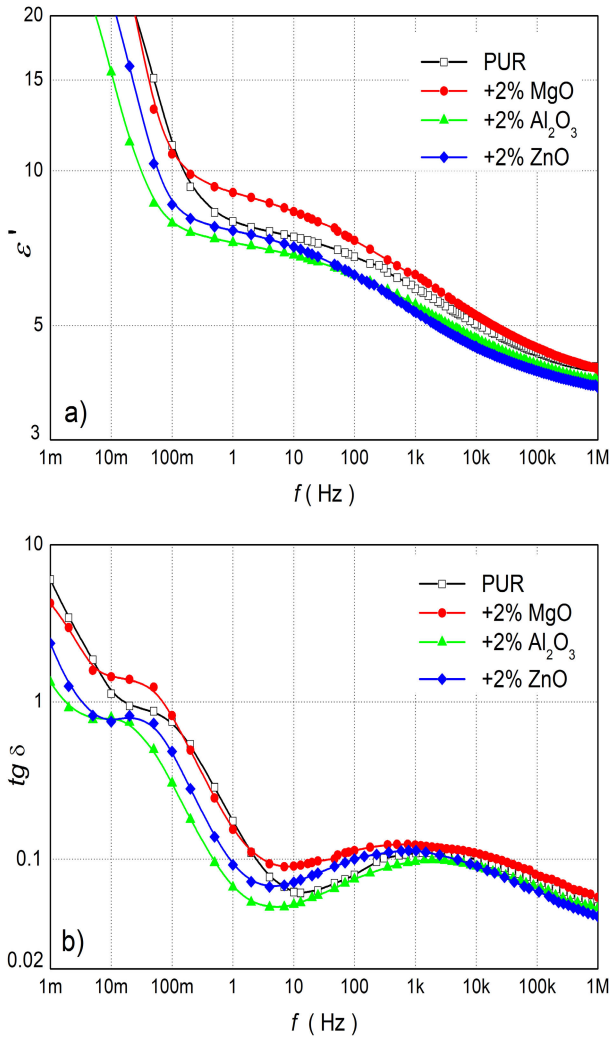

FIGURE 8. The frequency dependence of the real part of the complex relative permittivity (a) and tangent loss factor (b) for PUR with 2 wt.% concentrations of all investigated nanoparticles at 60 °C.

presence of a restriction in polymer chain mobility, a material loses its ability to relax at a given stress, resulting in a decrease in electrical polarization and permittivity (Fig. 7, 8). In layers around NPs are also trapped free charges, which caused an increase of a local electric field. This field reduced the influence of the external electric field, and there was a reduction in electric dipole motion in weaker field [39], [67], [68], [69]. Immobilized polymer chains and dipoles in the layers between the polymer matrix and the nanoparticles led to a decrease in the real permittivity for all nanocomposite except for the 2 wt.%. MgO. Only for the 2 wt.%. MgO (Fig. 8a) the higher real permittivity to that of pure PUR [35], [48] was observed, due to a dominant effect of MgO NPs with high real permittivity and freedom of polymer chains, tan δ was smaller than 0.2 (Fig 4b). Previous studies have shown that other polymer-based nanocomposites have similar properties.

From the DFS results, the tangent loss factor had two local maxima (Fig. 7b,d, e). At temperature (40 °C), only one maximum (f_1) was observed, which corresponds to *IDE* relaxation and is associated with bonding of polymer chains on the nanoparticles. With temperature, the thermal energy of the polymer chains increases, allowing them to oscillate with a higher frequency, which cause a decrease in the relaxation times (τ_1, τ_2) and therefore an increase in the eigenfrequencies (Table 3). Only in case of the 0.5 wt.% Al_2O_3 (Fig. 7b) the frequency shift to higher values was observed. The shift to lower frequencies, higher relaxation times, for 0.5 wt.% Al_2O_3, and 0.5 and 1.0 wt.% ZnO (Fig. 7b,f, 8b, Table 4) were observed. This was associated with a longer relaxation time due to generally lower polymer chain mobility and the local motion of the chain segment of the polar side groups around the C-C groups in the free volume of the outer level around the NP.

The second local maximum (f_2) was observable at frequencies below 1 Hz up to 40 °C and was related to α-relaxation relates to the glass transition temperature T_g and occurs due to the micro-Brownian motion of the entire polyurethane chains. The presence of 0.5 wt.% Al_2O_3 and 0.5 and 1.0 wt.% MgO NPs in nanocomposites caused its shift to higher eigenfrequencies compared to PUR (Fig. 7a). At 2.0 wt.% Al_2O_3 and MgO, all wt.% ZnO concentration (Fig. 8) there were a shift to lower eigenfrequencies (Table 4) what relate to the shift of tan δ to higher temperature (Fig. 4b) and higher T_g values for given concentrations (Table 4). Several previously published studies [70], [71],

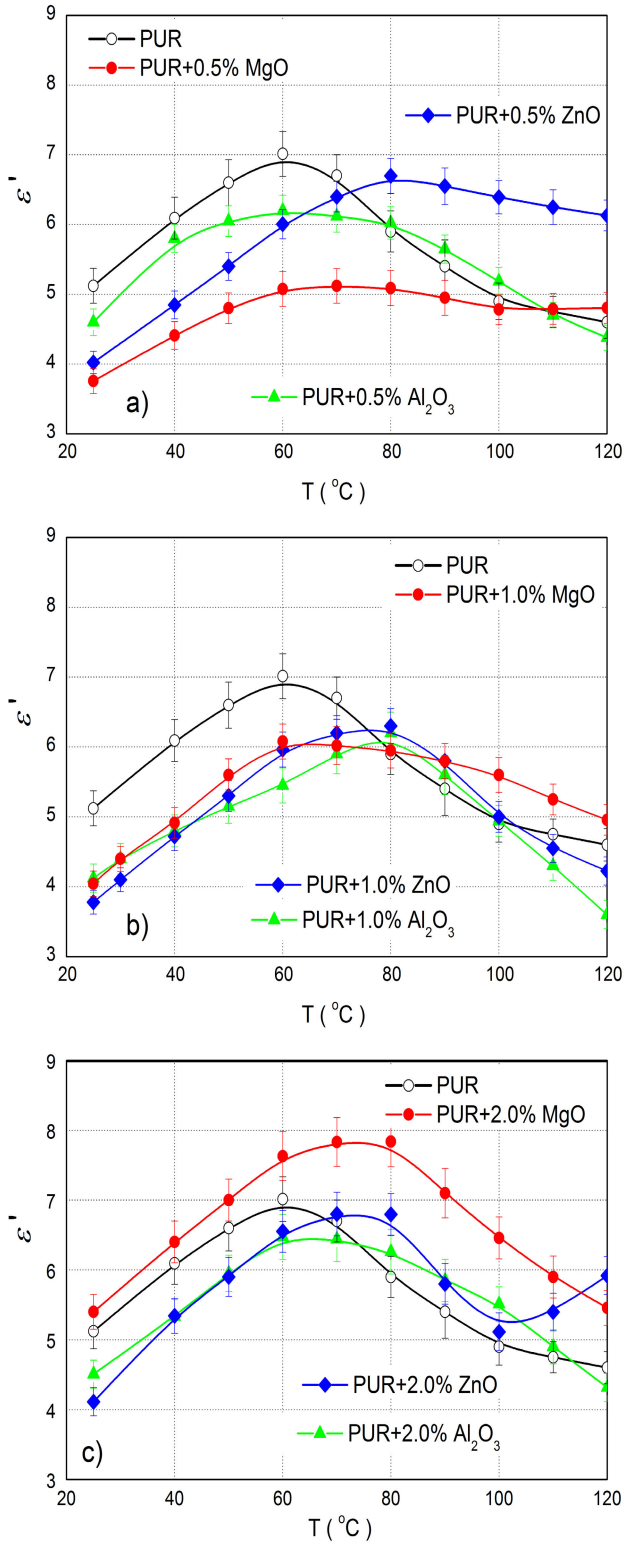

FIGURE 9. The temperature dependence of real part of the complex permittivity at 50 Hz for pure PUR and its mixture with various concentration of NPs.

[72], [73], [74] describe similar polyurethane's behavior in a temperature-frequency field, and the behavior was influenced by a variety of factors, including polymer chain mobility [54].

VI. CONCLUSION

In this research, we studied the effect of NPs on the dielectric properties of PUR. During the preparation of nanocomposites, polymer chains are attached to NPs in several layers. Due to these connections, their mobility changes significantly, which was reflected in the values of real permittivity and the development of polarization mechanisms (α, *IDE*). The decrease in the mobility of the polymer chains, which was confirmed by the DMA measurements up to a temperature of 60 °C, was also related to the measured decrease in the real permittivity for almost all the measurements. We observed an increase in the real permittivity over the whole temperature range only for the 2 wt.% MgO NPs in PUR. The presence of NPs and immobile polymers was also associated with a shift of the low eigenfrequency local maxima to lower frequencies at low concentrations and temperatures up to 60 °C.

Our future research efforts in this area will also focus on the systematic optimization of improving the mechanical and thermal properties of polymer nanocomposites in order to maximize their utility benefits just by incorporating nanoparticles.

REFERENCES

[1] A. Banerjee, N. Bose, and A. Lahiri, "Effect of zinc oxide nanofiller on the dielectric thermal and optical properties of polypropylene," *IEEE Trans. Ind. Appl.*, vol. 59, no. 1, pp. 479–485, Oct. 2023.

[2] G. Papalampris, P. Georgiou, T. Argyropoulos, E. Hristoforou, and P. Vassiliou, "Influence of ZnO (nano)rods on the dielectric properties of DGEBF epoxy exposed to progressive artificial weathering for VHF/early UHF applications," *Appl. Sci.*, vol. 13, no. 3, p. 1375, Jan. 2023.

[3] S. Maur, B. Chakraborty, A. K. Pradhan, S. Dalai, and B. Chatterjee, "A novel approach to estimate electrothermal aging of epoxy–alumina nanocomposites using dielectric relaxation current analysis," *IEEE Trans. Dielectr. Electr. Insul.*, vol. 30, no. 1, pp. 41–48, Feb. 2023.

[4] P. Bartko, M. Rajňák, R. Cimbala, K. Paulovičová, M. Timko, P. Kopčanský, and J. Kurimský, "Effect of electrical polarity on dielectric breakdown in a soft magnetic fluid," *J. Magn. Magn. Mater.*, vol. 497, Mar. 2020, Art. no. 166007.

[5] S. Utara, P. Jantachum, S. Hunpratub, N. Chanlek, and S. Phokha, "Enhanced dielectric constant and mechanical investigation of epoxidized natural rubber with TM-doped CeO_2 nanocomposites," *J. Alloys Compounds*, vol. 939, Apr. 2023, Art. no. 168601.

[6] S. El-Gamal and A. M. El Sayed, "Physical properties of the organic polymeric blend (PVA/PAM) modified with MgO nanofillers," *J. Compos. Mater.*, vol. 53, no. 20, pp. 2831–2847, Aug. 2019.

[7] A. Fouly, M. Taha, T. Albahkali, M. A. Shar, H. S. Abdo, and A. Nabhan, "Developing artificial intelligence models for predicting the tribo-mechanical properties of HDPE nanocomposite used in artificial hip joints," *IEEE Access*, vol. 12, pp. 14787–14799, 2024.

[8] A. Ersoy, F. Atalar, and H. Hiziroğlu, "A study on particle size effect of polyurethane-mica composites," *IEEE Access*, vol. 12, pp. 679–688, 2024.

[9] K. Parvathi and M. T. Ramesan, "Tailoring the structural, electrical and thermal properties of zinc oxide reinforced chlorinated natural rubber/poly (indole) blend nanocomposites for flexible electrochemical devices," *J. Polym. Res.*, vol. 30, no. 2, Feb. 2023, Art. no. 55.

[10] O. Faruqe, F. Haque, P. C. Saha, I. Jovanovic, N. Uzelac, and C. Park, "Partial incorporation of nonlinear resistive field grading materials: A strategy for enhanced field reduction and safety," *IEEE Trans. Dielectr. Electr. Insul.*, vol. 30, no. 1, pp. 474–483, Feb. 2023.

[11] H. Liu, Z. Bi, Z. Wan, X. Wang, Y. Wan, X. Guo, and Z. Cai, "Preparation and performance optimization of two-component waterborne polyurethane locomotive coating," *Coatings*, vol. 10, no. 1, p. 4, Dec. 2019.

[12] S.-H. Liu, M.-Y. Shen, C.-F. Kuan, H.-C. Kuan, C.-Y. Ke, and C.-L. Chiang, "Improving thermal stability of polyurethane through the addition of hyperbranched polysiloxane," *Polymers*, vol. 11, no. 4, p. 697, Apr. 2019.

[13] J. C. Q. Amado, E. Mustafa, and Z. A. Tamus, "Thermal resistance properties of polyurethanes and its composites," in *Thermosoftening Plastics*, G. A. Evingür, Ö Pekcan, and D. S. Achilias, Eds., London, U.K.: IntechOpen, 2019.

[14] J. Pagacz, E. Hebda, B. Janowski, D. Sternik, M. Jancia, and K. Pielichowski, "Thermal decomposition studies on polyurethane elastomers reinforced with polyhedral silsesquioxanes by evolved gas analysis," *Polym. Degradation Stability*, vol. 149, pp. 129–142, Mar. 2018.

[15] G. Polizos, E. Tuncer, A. L. Agapov, D. Stevens, A. P. Sokolov, M. K. Kidder, J. D. Jacobs, H. Koerner, R. A. Vaia, K. L. More, and I. Sauers, "Effect of polymer–nanoparticle interactions on the glass transition dynamics and the conductivity mechanism in polyurethane titanium dioxide nanocomposites," *Polymer*, vol. 53, no. 2, pp. 595–603, Jan. 2012.

[16] L. Jiang, Z. Ren, W. Zhao, W. Liu, H. Liu, and C. Zhu, "Synthesis and structure/properties characterizations of four polyurethane model hard segments," *Roy. Soc. Open Sci.*, vol. 5, no. 7, Jul. 2018, Art. no. 180536.

[17] L. Fetouhi, B. Petitgas, E. Dantras, and J. Martinez-Vega, "Mechanical, dielectric, and physicochemical properties of impregnating resin based on unsaturated polyesterimides," *Eur. Phys. J. Appl. Phys.*, vol. 80, no. 1, p. 10901, Oct. 2017.

[18] A. Alawy, A. Deshmukh, A. Le, and S. S. Park, "3D printed multifunctional polymeric nanocomposite components with sensing capability," *IEEE Access*, vol. 11, pp. 142577–142588, 2023.

[19] G. Polizos, E. Tuncer, V. Tomer, I. Sauers, C. A. Randall, and E. Manias, "Dielectric spectroscopy of polymer-based nanocomposite dielectrics with tailored interfaces and structured spatial distribution of fillers," in *Nanoscale Spectroscopy With Applications*, 2018, pp. 93–130.

[20] S. A. M. Abdelwahab, A. A. Salem, M. Shaban, and S. S. M. Ghoneim, "Maintenance enhancement of the performance of aged voltage transformers using nanoparticles," *IEEE Trans. Dielectr. Electr. Insul.*, vol. 31, no. 3, pp. 1628–1636, Jun. 2024.

[21] M. R. Atta, N. Algethami, M. O. Farea, Q. A. Alsulami, and A. Rajeh, "Enhancing the structural, thermal, and dielectric properties of the polymer nanocomposites based on polymer blend and barium titanate nanoparticles for application in energy storage," *Int. J. Energy Res.*, vol. 46, no. 6, pp. 8020–8029, May 2022.

[22] M. A. Subramanian, R. D. Shannon, B. H. T. Chai, M. M. Abraham, and M. C. Wintersgill, "Dielectric constants of BeO, MgO, and CaO using the two-terminal method," *Phys. Chem. Minerals*, vol. 16, pp. 741–746, Nov. doi: 10.1007/BF00209695.

[23] J. Kúdelčík, Š. Hardoň, P. Trnka, O. Michal, and J. Hornak, "Dielectric responses of polyurethane/zinc oxide blends for dry-type cast cold-curing resin transformers," *Polymers*, vol. 13, no. 3, p. 375, Jan. 2021.

[24] A. Soulintzis, G. Kontos, P. Karahaliou, G. C. Psarras, S. N. Georga, and C. A. Krontiras, "Dielectric relaxation processes in epoxy resin—ZnO composites," *J. Polym. Sci. B, Polym. Phys.*, vol. 47, no. 4, pp. 445–454, Feb. 2009.

[25] P. Jantachum, S. Phokha, S. Hunpratub, N. Chanlek, and S. Utara, "Improved cure characteristics and mechanical properties of an epoxidized natural rubber filled with cerium oxide nanoparticles: Influence of epoxide levels and filler loading," *J. Appl. Polym. Sci.*, vol. 141, no. 8, Feb. 2024, Art. no. e54969.

[26] S. Mallakpour and V. Behranvand, "Polymeric nanoparticles: Recent development in synthesis and application," *Exp. Polym. Lett.*, vol. 10, no. 11, pp. 895–913, 2016.

[27] O. Michal, V. Mentlik, and J. Hornak, "Impact of ultrasonic mixing on the electrical properties of PEI/SiO_2 nanocomposites," *AIP Conf. Proc.*, vol. 2411, no. 1, 2021, Art. no. 050010.

[28] Y. Xia, C. Zhou, G. Liang, A. Gu, and W. Wang, "Polyester-imide solventless impregnating resin and its nano-silica modified varnishes with excellent corona resistance and thermal stability," *IEEE Trans. Dielectr. Electr. Insul.*, vol. 22, no. 1, pp. 372–379, Feb. 2015.

[29] D. Torres-Torres, C. Torres-Torres, O. Vega-Becerra, J. C. Cheang-Wong, L. Rodríguez-Fernández, A. Crespo-Sosa, and A. Oliver, "Structured strengthening by two-wave optical ablation in silica with gold nanoparticles," *Opt. Laser Technol.*, vol. 75, pp. 115–122, Dec. 2015.

[30] F. Talbi, E. David, D. Malec, and D. Mary, "Dielectric properties of polyesterimide/SiO_2 nanocomposites," in *Proc. IEEE Conf. Electr. Insul. Dielectr. Phenomena (CEIDP)*, Richland, WA, USA, Oct. 2019, pp. 66–69.

[31] S. Okuzumi, Y. Murakami, M. Nagao, Y. Sekiguchi, C. C. Reddy, and Y. Murata, "DC breakdown strength and conduction current of MgO/LDPE composite influenced by filler size," in *Proc. Annu. Rep. Conf. Electr. Insul. Dielectr. Phenomena*, Quebec, QC, Canada, Oct. 2008, pp. 722–725.

[32] Y. Shen, J. Liu, Z. Li, J. Luo, S. Wang, J. Tang, P. Wang, D. Wang, X. Wang, X. Hu, and F. Zhang, "Preparation of functional ZnO nanoparticles and their application as UV photosensitizer and reinforcing agent for waterborne polyurethane acrylate composite coating," *J. Appl. Polym. Sci.*, vol. 140, no. 8, Feb. 2023, Art. no. e53528.

[33] E. A. Moawed, M. S. Eissa, and S. A. Al-Tantawy, "Application of polyurethane foam/zinc oxide nanocomposite for antibacterial activity, detection, and removal of basic dyes from wastewater," *Int. J. Environ. Sci. Technol.*, vol. 20, no. 7, pp. 7767–7774, Jul. 2023.

[34] J. Katayama, Y. Ohki, N. Fuse, M. Kozako, and T. Tanaka, "Effects of nanofiller materials on the dielectric properties of epoxy nanocomposites," *IEEE Trans. Dielectr. Electr. Insul.*, vol. 20, no. 1, pp. 157–165, Feb. 2013.

[35] D. F. Kavanagh, K. N. Gyftakis, and M. D. McCulloch, "Thermal degradation phenomena of polymer film on magnet wire for electromagnetic coils," *IEEE Trans. Ind. Appl.*, vol. 57, no. 1, pp. 458–467, Jan. 2021.

[36] R. Ramprasad, N. Shi, and C. Tang, "Modeling the physics and chemistry of interfaces in nanodielectrics," in *Dielectric Polymer Nanocomposites*, J. Nelson, Ed., Boston, MA, USA: Springer, 2010.

[37] VUKOL. *Material Safety Data Sheet*. [Online]. Available: https://www.vuki.sk/files/technickelisty/TDS-VUKOL-N22-sk.pdf

[38] J. Kúdelcík, Š. Hardon, P. Hockicko, M. Kúdelcíková, J. Hornak, P. Prosr, and P. Trnka, "Study of the complex permittivity of a polyurethane matrix modified by nanoparticles," *IEEE Access*, vol. 9, pp. 49547–49556, 2021.

[39] J. Hornak, P. Trnka, P. Kadlec, O. Michal, V. Mentlík, P. Šutta, G. M. Csányi, and Z. Á. Tamus, "Magnesium oxide nanoparticles: Dielectric properties, surface functionalization and improvement of epoxy-based composites insulating properties," *Nanomaterials*, vol. 8, no. 6, p. 381, May 2018.

[40] P. Havran, R. Cimbala, J. Kurimský, M. Rajňák, B. Dolník, D. Medved, and J. Király, "Dielectric relaxation response of electrical insulating liquids under different natures of thermal stress," *J. Mater. Res. Technol.*, vol. 25, pp. 1599–1611, Jul. 2023.

[41] J. Hornak, J. Černohous, P. Prosr, P. Rous, P. Trnka, A. Baran, and Š. Hardoň, "A comprehensive study of polyurethane potting compounds doped with magnesium oxide nanoparticles," *Polymers*, vol. 15, no. 6, p. 1532, Mar. 2023.

[42] L. Zhu, "Exploring strategies for high dielectric constant and low loss polymer dielectrics," *J. Phys. Chem. Lett.*, vol. 5, no. 21, pp. 3677–3687, Nov. 2014.

[43] NanoAmor. *Amorphous Aluminum Oxide Nanopowder, (γ-phase)*. [Online]. Available: https://nanoamor.com/inc/sdetail/60358

[44] NanoAmor. *Amorphous Products-Magnesium Oxide Nanopowder*. [Online]. Available: https://www.nanoamor.com/inc/sdetail/2543

[45] NanoAmor. *Amorphous Products-Zinc Oxide Nanopowder*. [Online]. Available: https://www.nanoamor.com/inc/sdetail/19983

[46] Š. Hardoň, J. Kúdelčík, A. Baran, O. Michal, P. Trnka, and J. Hornak, "Influence of nanoparticles on the dielectric response of a single component resin based on polyesterimide," *Polymers*, vol. 14, no. 11, p. 2202, May 2022.

[47] M. Wu, L. Lu, L. Yu, X. Yu, K. Naito, X. Qu, and Q. Zhang, "Preparation and characterization of epoxy/alumina nanocomposites," *J. Nanosci. Nanotechnol.*, vol. 20, no. 5, pp. 2964–2970, May 2020.

[48] R. Kochetov, "Thermal and electrical properties of nanocomposites, including material processing," Ph.D. thesis, Dept. Electr. Eng., Math. Comput. Sci., Saint-Petersburg State Electrotechnical Univ., Saint Petersburg, Russia, 2012.

[49] X. Qi, Q. Tang, P. Liu, and J. Hu, "Finite element analyses of working principle of the ultrasonic needle-droplet-substrate system for multiple-function manipulation," in *Intelligent Robotics and Applications* (Lecture Notes in Computer Science), vol. 11741, H. Yu, J. Liu, L. Liu, Z. Ju, Y. Liu, and D. Zhou, Eds., 2019, pp. 227–233.

[50] S. Pradhan, J. Hedberg, E. Blomberg, S. Wold, and I. O. Wallinder, "Effect of sonication on particle dispersion, administered dose and metal release of non-functionalized, non-inert metal nanoparticles," *J. Nanopart. Res.*, vol. 18, no. 9, Sep. 2016, Art. no. 285.

[51] Š. Hardoň, J. Kúdelčík, A. Baran, and P. Hockicko, "Measurement of effect of ultrasonic mixing on the properties of polyurethane potting compounds doped with ZnO nanoparticles," in *Proc. 14th Int. Conf. Meas.*, Smolenice, Slovakia, May 2023, pp. 155–158.

[52] G. N. Tomara, A. P. Kerasidou, A. C. Patsidis, P. K. Karahaliou, G. C. Psarras, S. N. Georga, and C. A. Krontiras, "Dielectric response and energy storage efficiency of low content TiO_2-polymer matrix nanocomposites," *Compos. A, Appl. Sci. Manuf.*, vol. 71, pp. 204–211, Apr. 2015.

[53] Y. Ahmad, "Polymeric dielectric material," in *Dielectric Material*, M. A. Silaghi, Ed., London, U.K.: IntechOpen, 2011, doi: 10.5772/50638.

[54] L. A. Ramajo, A. A. Cristóbal, P. M. Botta, J. M. P. López, M. M. Reboredo, and M. S. Castro, "Dielectric and magnetic response of Fe_3O_4/epoxy composites," *Compos. A, Appl. Sci. Manuf.*, vol. 40, no. 4, pp. 388–393, Apr. 2009, doi: 10.1016/j.compositesa.2008.12.017.

[55] A. Kanapitsas, P. Pissis, J. L. G. Ribelles, M. M. Pradas, E. G. Privalko, and V. P. Privalko, "Molecular mobility and hydration properties of segmented polyurethanes with varying structure of soft- and hard-chain segments," *J. Appl. Polym. Sci.*, vol. 71, no. 8, pp. 1209–1221, Feb. 1999.

[56] M. Klampar and K. Liedermann, "Dielectric relaxation spectroscopy of epoxy resins with TiO_2, Al_2, O_3, WO_3 and SiO_2, nanofillers," in *Proc. IEEE Int. Symp. Electr. Insul.*, San Juan, PR, USA, Jun. 2012, pp. 637–640.

[57] T. Tanaka, "Dielectric nanocomposites with insulating properties," *IEEE Trans. Dielectr. Electr. Insul.*, vol. 12, no. 5, pp. 914–928, Oct. 2005.

[58] P. Debye, "Zur theorie der spezifischen warme," *Annalen der Physik*, vol. 344, no. 14, pp. 789–839, 1912.

[59] P. Debye, *Polar Molecules*. New York, NY, USA: The Chemical Catalog Company, 1929.

[60] K. S. Cole and R. H. Cole, "Dispersion and absorption in dielectrics I. Alternating current characteristics," *J. Chem. Phys.*, vol. 9, no. 4, pp. 341–351, Apr. 1941.

[61] D. W. Davidson and R. H. Cole, "Dielectric relaxation in glycerol, propylene glycol, and n-Propanol," *J. Chem. Phys.*, vol. 19, no. 12, pp. 1484–1490, Dec. 1951.

[62] K. Górska, A. Horzela, L. Bratek, G. Dattoli, and K. A. Penson, "The Havriliak–Negami relaxation and its relatives: The response, relaxation and probability density functions," *J. Phys. A, Math. Theor.*, vol. 51, no. 13, Apr. 2018, Art. no. 135202.

[63] C. Gherasim, M. Asandulesa, N. Fifere, F. Doroftei, D. Tîmpu, and A. Airinei, "Structural, optical and dielectric properties of some nanocomposites derived from copper oxide nanoparticles embedded in poly(vinylpyrrolidone) matrix," *Nanomaterials*, vol. 14, no. 9, p. 759, Apr. 2024.

[64] J. Miao, M. Dong, M. Ren, X. Wu, L. Shen, and H. Wang, "Effect of nanoparticle polarization on relative permittivity of transformer oil-based nanofluids," *J. Appl. Phys.*, vol. 113, no. 20, May 2013, Art. no. 204103.

[65] T. Tanaka, G. C. Montanari, and R. Malhaupt, "Process, understanding and challenges in the field of nanodielectrics," *IEEE Trans. Dielectr. Electr. Insul*, vol. 11, no. 5, pp. 763–784, 2004.

[66] M. Watanabe and T. Hirai, "Space charge distribution in bending-electrostrictive polyurethane films doped with salts," *J. Polym. Sci. B, Polym. Phys.*, vol. 42, no. 3, pp. 523–531, Feb. 2004.

[67] S. Awad, A. Al-Rashdi, E. Abdel-Hady, Y. Jean, and J. D. Van Horn, "Free volume properties of the zinc oxide nanoparticles/waterborne polyurethane coating system studied by a slow positron beam," *J. Compos. Mater.*, vol. 53, no. 13, pp. 1765–1775, Jun. 2019.

[68] P. Pissis, "Molecular dynamics of thermoset nanocomposites," in *Thermoset Nanocomposites for Engineering Application*. Shropshire, U.K.: Smithers Rapra Technology, 2007, pp. 143–206.

[69] G. Boiteux, G. Seytre, L. Cuve, and J.-P. Pascault, "Dielectric studies of segmented polyurethanes based on polyolefine: Relations between structure and dielectric behaviour," *J. Non-Crystalline Solids*, vols. 131–133, pp. 1131–1135, Jun. 1991.

[70] L. V. Karabanova, G. Boiteux, O. Gain, G. Seytre, L. M. Sergeeva, and E. D. Lutsyk, "Semiinterpenetrating polymer networks based on polyurethane and polyvinylpyrrolidone. I. Thermodynamic state and dynamic mechanical analysis," *J. Appl. Polym. Sci.*, vol. 80, no. 6, pp. 852–862, 2001.

[71] S. A. Madbouly and M. R. Kessler, "Dielectric spectroscopy for biorenewable plant oil-based polyurethane," in *Proc. IEEE Conf. Electr. Insul. Dielectric Phenomena (CEIDP)*, Oct. 2014, pp. 788–791.

[72] Y. V. Savelyev, E. R. Akhranovich, A. P. Grekov, E. G. Privalko, V. V. Korskanov, V. I. Shtompel, V. P. Privalko, P. Pissis, and A. Kanapitsas, "Influence of chain extenders and chain end groups on properties of segmented polyurethanes. I. Phase morphology," *Polymer*, vol. 39, no. 15, pp. 3425–3429, Jul. 1998.

[73] M. Gutten, D. Korenčiak, M. Karman, P. Brncal, M. Kucera, T. N. Koltunowicz, and M. Sulowicz, "Combination of non-contact and contact measuring methods for analyzing structural conditions of dry transformers," *Meas. Sci. Rev.*, vol. 23, no. 4, pp. 154–162, Aug. 2023.

[74] Y. Yu, Y. Zhao, B. Huang, Y. Ji, Y. Zhao, Z. Zhang, and H. Fei, "Dielectric properties and dielectric relaxation process of polymethylphenylsiloxane/silicon dioxide nanocomposites," *J. Appl. Polym. Sci.*, vol. 139, no. 31, Aug. 2022, Art. no. e52716, doi: 10.1002/app.52716.

ŠTEFAN HARDOŇ was born in 1988. He received the degree from the Department of Telecommunication, University of Žilina, and the Ph.D. degree in electrotechnologies and materials, in 2015, with focusing exploitation of acoustic techniques at research materials and structures. Since 2015, he has been a Researcher with the Department of Physics, University of Žilina. His current research interests include processes in electroinsulating materials, and study and research of impact of nanoparticles od dielectric properties of new modern progressive materials. Acoustic and dielectric spectroscopy are used in his research techniques.

JOZEF KÚDELČÍK was born in Ružomberok, Slovakia, in January 1975. He received the Mgr. degree from the Department of Plasma Physics, Faculty of Mathematics and Physics, Comenius University in Bratislava, in 1998, and the Ph.D. degree in stage of breakdown in the mixtures with SF6, in 2003. In 2011, he habilitated in electrotechnology and materials. Since 1998, he has been a Researcher with the Department of Physics, University of Žilina. His scientific research is focused to discharge mechanism and partial discharge in gases and dielectric, such as water or oil. His second great area of research is the processes in magnetic fluids, liquid crystals, and nanocomposites in a magnetic field studied by acoustic and dielectric spectroscopy.

ANTON BARAN was born in Košice, Slovakia, in May 1982. He received the master's and Ph.D. degrees from the Faculty of Science, Pavol Jozef Šafarik University in Košice. Since 2013, he has been an Assistant Professor with the Department of Physics, Technical University of Košice. His current research interests include structure, morphology, and relaxation processes in synthetic, and biodegradable polymers.

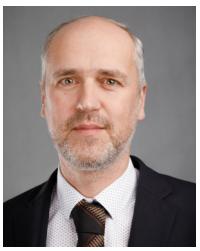

PAVEL TRNKA (Senior Member, IEEE) received the M.Sc. and Ph.D. degrees from the University of West Bohemia, Czech Republic, in 2002 and 2005, respectively, and the Dr. hab. degree from the Faculty of Electrical Engineering, University of Žilina, Slovakia, in 2008. He was a Student of the University of Applied Science, Fachhochschule, Regensburg, Germany, and the Department of Research, Maschienenenfabrik Reinhausen, Germany, in 2003 and 2004. From 2006 to 2007, he was a Postdoctoral Associate with the High Voltage Laboratory, Department of Electrical and Computer Engineering, Mississippi State University. He is a DEIS Member, a member of the Executive Committee of the Czechoslovakia Section IEEE, and the Chairman of CDEE 2020.

ONDREJ MICHAL (Member, IEEE) was born in 1993. He received the master's and Ph.D. degrees from the University of West Bohemia, in 2017 and 2021, respectively. Since the bachelor's thesis, he has specialized in the field of nanocomposite materials. His research primarily focuses on the development of new electrical insulation materials, focusing on characterizing their physical properties he is also interested in sustainability in this field. Additionally, he heavily focuses on the application of automation techniques in diagnostics. He is a member of the IEEE Young Professionals and the IEEE Dielectrics and Electrical Insulation Society.

ADAM TAMUS (Member, IEEE) received the M.Sc., Ph.D., and Habilitation degrees in electrical engineering from Budapest University of Technology and Economics, Hungary, in 1997, 2011, and 2019, respectively. Since 2001, he has been associated with the Department of Electric Power Engineering, Faculty of Electrical Engineering and Informatics, Budapest University of Technology and Economics, where he has been an Associate Professor. He has more than 90 research articles to his name. His research interests include electrical insulation technology, insulation diagnostics, electrical characterization, electrical breakdown, and health effects of electromagnetic fields.

TOMASZ KOLTUNOWICZ was born in Opatow, Poland, in 1979. He received the M.Sc. Eng. degree in electrical engineering and the Ph.D. and D.Sc. degrees in scientific discipline of electrical engineering from Lublin University of Technology, in 2004, 2011, and 2016, respectively. His research interests include electrical properties of nanocomposites (materials science) and paper-oil insulation in power transformers (electrical engineering), and developing new methods of determining moisture content in solid-liquid insulation.

ALENA KOZÁKOVÁ was born in 1977. She received the degree from the Faculty of Chemical Technology, Department of Organic Technologies and Petrochemistry, Slovak Technical University in Bratislava. She is currently engaged in research and development of ecological electro-insulating varnishes and resins for the electrochemical industry.

TOMÁŠ DÉRER was born in 1966. He received the University Education degree in organic chemistry from the Faculty of Chemical Technology, Slovak Technical University in Bratislava. He is currently engaged in research and development of polyurethane-based potting compounds used in the electrical industry.

JAROSLAV HORNAK (Senior Member, IEEE) was born in Klatovy, in 1989. He received the master's and Ph.D. degrees from the University of West Bohemia, Czech Republic, in 2014 and 2018, respectively. He completed a Traineeship with P&G Rakona, Rakovník, Czech Republic, in 2016, and a Practical Internship with the Faculty of Electrical Engineering, University of Žilina, Žilina, Slovakia, in 2017 and 2022. His research interests include research and development in the area of dielectric materials and diagnostics of their interactions with an electric field. He is an IEEE DEIS Member, a member of the Executive Committee of the IEEE Czechoslovakia Section, and the Chair of IEEE Young Professionals CS AG.